Development of a visible-light-responsive titania nanotube photocatalyst by site-selective modification with hetero metal ions

著者	Murakami Naoya, Fujisawa Yuichi, Tsubota Toshiki, Ohno Teruhisa
journal or publication title	Applied Catalysis B: Environmental
volume	92
number	1-2
page range	56-60
year	2009-10-19
URL	http://hdl.handle.net/10228/00006576

doi: info:doi/10.1016/j.apcatb.2009.07.023

Development of a visible light-responsive titania nanotube photocatalyst by site-selective modification with hetero metal ions

Naoya Murakami, Yuichi Fujisawa, Toshiki Tsubota and Teruhisa Ohno*

Department of Applied Chemistry, Faculty of Engineering, Kyushu Institute of Technology, 1-1 Sensuicho, Tobata, Kitakyushu 804-8550, Japan

Keywords

Visible light responsive photocatalyst, Titania nanotube, Site-selective modification of metal ion

Abstract

A titania nanotube (TNT), which was obtained by calcinations of a titanate nanotube, was modified with two kinds of transition metal ions, iron(III) (Fe^{3+}) and zinc(II) (Zn^{2+}) ions. TNT with site-selective modification with metal ions showed higher photocatalytic activity than that of bare TNT, presumably due to separation of redox sites, and oxidation on the outside surface and reduction on the inside surface were the preferable separated redox sites on the tubular structure for decomposition of acetaldehyde. Modification of TNT with Fe^{3+} ions induced improvement of photocatalytic activity under visible-light irradiation as well as ultraviolet (UV) irradiation. On the other hand, TNT modified with Zn^{2+} ions showed the largest enhancement of photocatalytic activity under UV irradiation, though increase in visible-light activity was hardly observed. Double-beam photoacoustic spectroscopic analyses indicated that Zn^{2+} ion works efficiently as an electron acceptor, while Fe^{3+} ion is an effective sensitizer for visible light.

* Corresponding author. TEL/FAX: +81-93-884-3318

E-mail address: tohno@che.kyutech.ac.jp (T. Ohno)

1. Introduction

One-dimensional nanomaterials, e.g., nanofiber, nanorod and nanotube, have been intensively studied for applications to nanodevices. A titanate nanotube, which is obtained by a simple soft chemical process [1,2], has a nanometer-sized diameter and length of a few hundred nanometers. Various applications of titanate nanotube, including applications to dye-sensitized solar cell [3], hydrogen storage [4] and catalyst support [5,6], have been realized by utilization of its characteristic geometrical structure, e.g., tubular structure and large specific surface area.

For application as a photocatalyst, a titanate nanotube has sometimes been thermally treated in order to improve its chemical, physical and mechanical stability and its crystallinity by crystal transformation into titanium(IV) oxide (TiO_2). TiO_2 is an attractive material as a photocatalyst due to its super redox ability, availability and non-toxicity [7,8], though it works only under ultraviolet (UV) irradiation. For improvement of photocatalytic activity, nanoparticles with large specific surface areas are frequently used because of the large number of reaction sites, and several groups have studied the photocatalytic activity of titanate-related materials with large specific surface areas [9,10].

Another possible method for enhancement of photocatalytic activity is separation of redox sites, because redox reactions in neighboring sites sometimes induce back reaction, resulting in decline of photocatalytic efficiency. Therefore, separation of electrons and positive holes from each other might enable photocatalytic efficiency to be improved by utilization of the geometrical structure and a cocatalyst. Our group has demonstrated the availability of a titania nanotube (TNT) as a reaction-site-separated photocatalyst by site-selective deposition of platinum (Pt) nanoparticles as reduction catalysts [11]. TNT with site-selective deposition of Pt on the inside/outside surface of the nanotube showed a higher photocatalytic activity than that of conventional spherical particles and that of TNT with non-site-selective deposition because site-selective deposition presumably induced separation of redox sites between the inside and outside surfaces of TNT. In further study, this method was applied to modification of Fe^{3+} ion on sulfur-doped TNT (S-TNT), which exhibited photocatalytic activity under visible-light irradiation

[12], and S-TNT with site-selective modification of Fe^{3+} ion showed improvement of photocatalytic activity under visible-light irradiation as well as UV irradiation. This and subsequent study indicate that Fe^{3+} ion works as a sensitizer for visible light as well as an electron acceptor [12-14].

In the present study, visible-light activity of non-doped TNT was improved by site-selective-modification of Fe^{3+} ion, which acts as a sensitizer for visible light. The surface of TNT was also site-selectively modified with Zn^{2+} ion, which is expected to work as an effective electron acceptor.

2. Experimental

2.1 Material and instruments

TNT with anatase crystal structure of TiO_2 was obtained by 5 h of calcinations of titanate nanotube powders (TNT-365, Catalysts & Chemicals Ind. Co., Ltd.) at 350 °C. The crystal structures of the powders were confirmed by using an X-ray diffractometer (Rigaku, MiniFlex II) with Cu K□ radiation (□= 1.5405 Å). The tubular structure was maintained after calcination, as shown by observation using a transmission electron microscope (TEM; Hitachi, H-9000NAR). Modification of TNT with a transition metal ion was performed by three procedures as described in the following sections. The amount of metal ions on the surface of TNT was estimated by analysis of residue of metal ions by inductively coupled plasma optical emission spectroscopy (IPC; Shimadzu, ICPS-8000). The diffuse reflectance (DR) spectra were measured using a Shimadzu UV-2500PC spectrophotometer equipped with an integrating sphere unit (ISR-240A).

2.2 Modification of the entire surface of TNT with transition metal ions

Before modification transition metal ions, the TNT was dried under reduced pressure at 100 °C for 2 h in order to remove physisorbed water inside TNT. An aqueous suspension composed of TNT and an aqueous solution of iron(III) nitrate enneahydrate ($Fe(NO_3)_3 \cdot 9H_2O$) and zinc(II) chloride ($ZnCl_2$), the amount of which corresponds to 1 wt% modification of metal ions, was stirred for 3 h under an aerated condition. After filtration, the particles were dried under

reduced pressure at 60 °C for 3 h, and then TNT samples with non-site-selective modification of Fe^{3+} and Zn^{2+} on the entire surface (e-Fe^{3+}, e-Zn^{2+}) were obtained.

2.3 Modification of the inside surface of TNT with transition metal ions

Before modification with transition metal ions, the TNT was dried under reduced pressure at 100 °C for 2 h in order to remove physisorbed water inside the TNT. An aqueous suspension composed of TNT and an aqueous solution of $Fe(NO_3)_3$ and $ZnCl_2$, the amount of which corresponds to 3 wt% modification of metal, was stirred for 3 h under an aerated condition. After filtration, transition metal ions on the outside surface of TNT were removed by washing with 1 mol dm^{-3} of aqueous solution of hydrochloric acid. By this procedure, the amount of metal ion on TNT was decreased to ca. 1 wt%. The particles were dried under reduced pressure at 60 °C for 3 h, and then TNT samples with site-selective modification of Fe^{3+} and Zn^{2+} on the inside surface (i-Fe^{3+}, i-Zn^{2+}) were obtained.

2.4 Modification of the outside surface of TNT with transition metal ions

TNT powders were spread on the bottom of a glass dish and sprayed with an aqueous solution of $Fe(NO_3)_3$ and $ZnCl_2$, the amount of which corresponds to 1 wt% modification of metal ions, and dried under reduced pressure. The particles were dried under reduced pressure at 60 °C for 3 h, and then TNT samples with site-selective modification of Fe^{3+} and Zn^{2+} on the outside surface (o-Fe^{3+}, o-Zn^{2+}) were obtained

2.5 Photocatalytic decomposition over acetaldehyde

Photocatalytic activities of TNT samples were evaluated by photocatalytic decomposition over acetaldehyde. One hundred milligrams of TNT powder, which has a complete extinction of the incident radiation, was spread on a glass dish, and the glass dish was placed in a 125 cm^3 Tedlar bag (AS ONE Co. Ltd.). Five hundred parts per million of gaseous acetaldehyde was injected into the Tedlar bag, and photoirradiation was performed at room temperature after the acetaldehyde had

reached adsorption equilibrium. The gaseous composition in the Tedlar bag was 79% of N_2, 21% of O_2, < 0.1 ppm of CO_2 and 500 ppm of acetaldehyde, and relative humidity was ca. 30%. A 500-W xenon lamp (Ushio, SX-UI501XQ) was used as a light source and the wavelength of photoirradiation was controlled by UV-35 and L-42 filters (Asahi Techno Glass Co.), and an intensity of 12 mW cm^{-2} was used as the light source. The concentrations of acetaldehyde and carbon dioxide (CO_2) were estimated by gas chromatography (Shimadzu, GC-8A, FID detector) with a PEG-20 M 20% Celite 545 packed glass column and by gas chromatography (Shimadzu, GC-9A, FID detector) with a TCP 20% Uniport R packed column and a methanizer (GL Sciences, MT-221), respectively. In the photocatalytic evaluation, P-25 (Japan Aerosil Co., S_{BET} = 50 m^2 g^{-1}), which is a well-known commercial TiO_2 photocatalyst with a high photocatalytic activity, was employed as a standard photocatalyst.

2.6 Double-beam photoacoustic spectroscopic measurement

A gas-exchangeable photoacoustic (PA) cell equipped with two valves for gas flow was used, and a TiO_2 sample was placed in the cell. The atmosphere was controlled by a flow of N_2 containing ethanol vapor (N_2 + EtOH), and the measurements were conducted after shutting off the valves, i.e., in a closed system at room temperature. A light-emitting diode (LED) emitting light at ca. 625 nm (Luxeon LXHL-ND98) was used as a probe light, and the output intensity was modulated by a digital function generator (NF DF1905) at 80 Hz. In addition to the modulated light, a blue-LED (Luxeon LXHL-NB98, emitting light at ca. 470 nm, 8.1 mW cm^{-2}) was also used as simultaneous continuous irradiation for photoexcitation. The PA signal acquired by a condenser microphone buried in the cell was amplified and monitored by a digital lock-in amplifier (NF LI5640). Detailed setups of double-beam photoacoustic (DB-PA) spectroscopic measurements have been reported previously [15].

3. Results and discussion

3.1 Photoabsorption properties of metal-ion-modified TNT

Photoabsorption of TNT changed due to modification with metal ions. Figure 1 shows DR spectra of bare TNT, e-Zn^{2+} and e-Fe^{3+}. Appreciable dependence of photoabsorption on the modification site of metal ions was not observed. Modification of Fe^{3+} on TNT induced an increase of photoabsorption in the wavelength region of 400~550 nm, but only small increase was observed on Zn^{2+}-modified TNT. Net amounts of modified Fe^{3+} ions were 1.0 wt%, 1.0 wt%, and 0.88 wt% for e-Fe^{3+}, o-Fe^{3+} and i-Fe^{3+}, while net amounts of modified Zn^{2+} ions were 0.95 wt%, 0.96 wt% and 0.81 wt% for e-Zn^{2+}, o-Zn^{2+} and i-Zn^{2+}, respectively. These results indicate that the reason for the small photoabsorption of e-Zn^{2+} was not the small amount of Zn^{2+} modification on TNT but the small photoabsorption of Zn^{2+} on TNT in the visible-light region.

3.2 Photocatalytic reaction of TNT with non-site-selective and site-selective modification with Fe^{3+} ions under visible-light irradiation

Figure 2 shows the time courses of CO_2 evolution of acetaldehyde decomposition over bare TNT, i-Fe^{3+}, e-Fe^{3+} and o-Fe^{3+} under visible-light irradiation. Fe^{3+}-modified TNT showed higher photocatalytic activity than that of bare TNT under visible-light irradiation. We previously reported that modification of rutile TiO_2 with a transition metal ion, such as Fe^{3+} and Cu^{2+}, induced photocatalytic activity under visible-light irradiation by working as a sensitizer for visible light [13]. Therefore, Fe^{3+} ions on anatase TNT are also thought to absorb visible light and induce photocatalytic reaction. Although dependence of photoabsorptiopn of Fe^{3+}-modified TNT on modification site was not observed, photocatalytic activity under visible-light irradiation depended on modification sites of Fe^{3+} ions (o-Fe^{3+} > e-Fe^{3+} > i-Fe^{3+} > bare). This indicates that modification sites have a great influence on photocatalytic activity.

DB-PA measurements were carried out in order to estimate the amount of electrons injected into TiO_2 by detecting photogenerated trivalent titanium (Ti^{3+}) species on TiO_2 particles [13]. Figure 3 shows time-course curves of PA signals of bare TNT, i-Fe^{3+}, e-Fe^{3+} and o-Fe^{3+} under visible-light irradiation in the presence of N_2 + EtOH. The PA signal of Fe^{3+}-modified TNT was increased by photoirradiation of ca. 470 nm and was larger than that of bare TNT. The mechanism

of Ti^{3+} generation can be explained as follows: (1) photoexcited metal ions (M^{n+}) injected electrons into TiO_2 and became an oxidized state ($M^{(n+1)+}$), (2) injected electrons reduced Ti^{4+} to Ti^{3+} and (3) the oxidized state of metal ions ($M^{(n+1)+}$) oxidized ethanol to go back to the initial state of metal ions (M^{n+}) [13].

The amount of injected electrons estimated from the time-course curve of PA signals showed a close relationship with photocatalytic activity as shown in Fig. 2 (o-Fe^{3+} > e-Fe^{3+} > i-Fe^{3+} > bare). This indicates that photocatalytic activity is determined by amount of injected electrons and that Fe^{3+} modification of the outside surface induces more effective electron injection than does modification of the inside surface. The reason for it is thought to be the difference in adsorption properties, such as surface area and diffusion of the substrate (acetaldehyde for photocatalytic evaluation and ethanol for DB-PA analysis) between the outside and inside surfaces of TNT. The molecular size of acetaldehyde or ethanol, which is a substrate for oxidation, is much larger than that of oxygen working as an electron acceptor. Thus, diffusion-controlled oxidation of the substrate was more likely to occur on the outside surface of TNT than on the inside surface, and oxidation reaction on the outside surface and reduction reaction on the inside surface were preferable. This tendency agrees with the results of our previous study on S-TNT modified with Fe^{3+} ions, which showed high photocatalytic activity under visible-light irradiation [12].

3.3 Photocatalytic reaction of TNT with non-site-selective and site-selective modification with Zn^{2+} ions under visible-light irradiation

Photocatalytic activity of TNT with site-selective modification of Zn^{2+} ions was also studied. Figure 4 shows the time course of CO_2 evolution of acetaldehyde decomposition over bare TNT, i-Zn^{2+}, e-Zn^{2+} and o-Zn^{2+} under visible-light irradiation. Zn^{2+} modification also induced photocatalytic activity under visible-light irradiation and similar dependence of modification site on photocatalytic activity was seen (o-Zn^{2+} > e-Zn^{2+} > i-Zn^{2+} > bare). However, its activity was about one-third of that of Fe^{3+}-modified TNT.

Figure 5 shows time-course curves of PA signals of bare TNT, i-Zn^{2+}, e-Zn^{2+} and o-Zn^{2+}

under visible-light irradiation in the presence of N_2 + EtOH. PA signal of Zn^{2+}-modified samples also increased with visible-light irradiation and the increase showed dependence on modification sites. However, saturation of the PA signal was smaller than that of Fe^{3+}-modified samples. This result agrees with the photocatalytic activity, indicating that Zn^{2+} ion hardly works as a sensitizer for visible light because of the small photoabsorption as observed in DR spectra (Fig. 1).

3.4 Photocatalytic reaction of TNT with non-site-selective and site-selective modification with Zn^{2+} ions under UV irradiation

Although Zn^{2+}-modified TNT showed lower activity than that of Fe^{3+}-modified TNT under visible-light irradiation, modification with Zn^{2+} greatly enhanced the photocatalytic activity under UV irradiation. Figure 6 shows the time course of CO_2 evolution of acetaldehyde decomposition over bare TNT, e-Zn^{2+}, o-Zn^{2+}, i-Zn^{2+} and i-Fe^{3+} under UV irradiation. All of the metal-ion-modified TNT samples showed higher photocatalytic activity than that of bare TNT. The results of our previous study indicated that some kinds of transition metal ions enhance photocatalytic activity by working as electron acceptors under the above bandgap photoirradiation [13]. i-Zn^{2+} also showed higher activity than that of bare TNT and i-Fe^{3+}. This suggests that Zn^{2+} ion also work as a more effective electron acceptor than Fe^{3+} ion.

Dependence of the modification site of Zn^{2+} was observed for photocatalytic activity also under UV irradiation. i-Zn^{2+} showed higher photocatalytic activity under UV irradiation than that of o-Zn^{2+}, in contrast to the photocatalytic activity under visible-light irradiation. Under UV irradiation, reduction is mainly thought to proceed on metal Zn^{2+} and Fe^{3+} because Zn^{2+} and Fe^{3+} ions presumably work as electron acceptors. Therefore, preferable separated redox sites on metal-ion-modified TNT under UV irradiation are the same as those under visible-light irradiation: the inside and outside surfaces of TNT are preferable sites for reduction and oxidation, respectively.

3.4 Photocatalytic reaction of TNT with site-selective modification with Zn^{2+} and Fe^{3+} ions under visible-light irradiation

Results of photocatalytic evaluation and PA analyses indicate that Fe^{3+} ion was an effective sensitizer for visible light, while Zn^{2+} works as an efficient electron acceptor. Therefore, site-selective modification was carried out using two kinds of transition metal ions with different roles: Fe^{3+} ions for site-selective modification of the outside surface of TNT after site-selective modification of the inside surface of TNT with Zn^{2+}. This TNT sample is denoted by o-Fe^{3+}/i-Zn^{2+}.

Figure 7 shows the time courses of CO_2 evolution of acetaldehyde decomposition over bare TNT, i-Zn^{2+}, o-Fe^{3+} and o-Fe^{3+}/i-Zn^{2+} under visible-light irradiation. The results indicate that o-Fe^{3+}/i-Zn^{2+} had higher photocatalytic activity than that of o-Fe^{3+}. One plausible reason for this is that Zn^{2+} prevents injected electrons from going back to the Fe^{4+} state by working as an electron acceptor.

Figure 8 shows time-course curves of PA signals of bare TNT, i-Zn^{2+}, o-Fe^{3+} and o-Fe^{3+}/i-Zn^{2+} under visible-light irradiation in the presence of N_2 + EtOH. The slower increase of the PA signal in o-Fe^{3+}/i-Zn^{2+} than that of o-Fe^{3+} in the initial period of photoirradiation suggests that injected electrons were consumed by Zn^{2+} ions on the inside surface of TNT. On the other hand, saturation of the PA signal of o-Fe^{3+}/i-Zn^{2+} approached a value similar to that of o-Fe^{3+} with a longer duration of photoirradiation because electrons accumulated in TNT after saturation of the electron-accepting capacity of Zn^{2+} ions.

Conclusion

Modification with a metal ion improved photocatalytic activity for acetaldehyde decomposition as a result of separation of redox sites between the inside and outside surfaces of TNT. The outside surface of TNT was the preferable oxidation site under visible-light irradiation, because oxidation of acetaldehyde decomposition was a diffusion-controlled reaction on the inside surface of TNT. Fe^{3+} ion worked as an electron acceptor as well as a sensitizer, but Zn^{2+} ion exhibited higher ability as an electron acceptor than a sensitizer for visible light. The o-Fe^{3+}/i-Zn^{2+} sample showed the highest visible-light activity among the metal-ion-modified TNT samples

because injected electrons from Fe^{3+} ions on the outside surface of TNT migrated to Zn^{2+} ions on the inside surface of TNT without being consumed by back electron transfer.

Acknowledgement

This work was supported by a grant of Knowledge Cluster Initiative implemented by the Ministry of Education, Culture, Sports, Science and Technology (MEXT) and the New Energy and Industrial Technology Development Organization (NEDO).

Figures and captions

Figure 1. DR spectra of (a) bare TNT, (b) e-Zn^{2+} and (c) e-Fe^{3+}.

Figure 2. Time courses of CO_2 evolution of acetaldehyde decomposition over (a) bare TNT, (b) i-Fe^{3+}, (c) e-Fe^{3+} and (d) o-Fe^{3+} under visible-light irradiation (λ_{ex} > 420 nm, I = 12 mW cm^{-2}).

Figure 3. Time-course curves of PA signals of (a) bare TNT, (b) i-Fe^{3+}, (c) e-Fe^{3+} and (d) o-Fe^{3+} under visible-light irradiation (λ_{ex} = 470 nm, I = 8.1 mW cm^{-2}) in the presence of N_2 + EtOH.

Figure 4. Time courses of CO_2 evolution of acetaldehyde decomposition over (a) bare TNT, (b) i-Zn^{2+}, (c) e-Zn^{2+} and (d) o-Zn^{2+} under visible-light irradiation (λ_{ex} > 420 nm, I = 12 mW cm^{-2}).

Figure 5. Time-course curves of PA signals of (a) bare TNT, (b) i-Zn^{2+}, (c) e-Zn^{2+}, (d) o-Zn^{2+} and (e) o-Fe^{3+} under visible-light irradiation (λ_{ex} = 470 nm, I = 8.1 mW cm^{-2}) in the presence of N_2 + EtOH.

Figure 6. Time courses of CO_2 evolution of acetaldehyde decomposition over (a) bare TNT, (b) e-Zn^{2+}, (c) o-Zn^{2+}, (d) i-Zn^{2+} and (e) i-Fe^{3+} under UV irradiation (λ_{ex} > 350 nm, I = 12 mW cm^{-2}).

Figure 7. Time courses of CO_2 evolution of acetaldehyde decomposition over (a) bare TNT, (b) i-Zn^{2+}, (c) o-Fe^{3+} and (d) o-Fe^{3+}/i-Zn^{2+} under visible-light irradiation (λ_{ex} > 420 nm, I = 12 mW cm^{-2}).

Figure 8. Time-course curves of PA signals of (a) bare TNT, (b) i-Zn^{2+}, (c) o-Fe^{3+} and (d) o-Fe^{3+}/i-Zn^{2+} under visible-light irradiation (λ_{ex} = 470 nm, I = 8.1 mW cm^{-2}) in the presence of N_2 + EtOH.

References

[1] T. Kasuga, M. Hiromatsu, A. Hoson, T. Sekino, K. Niihara, Langmuir 14 (1998) 3163.

[2] T. Kasuga, M. Hiramatsu, A. Hoson, T. Sekino, K. Niihara, Adv. Mater. 11 (1999) 1307.

[3] S. Uchida, R. Chiba, M. Tomiha, N. Masaki, M. Shirai, Electrochemistry 70 (2002) 418.

[4] D.V. Bavykin, A.A. Lapkin, P.K. Plucinski, J.M. Friedrich, F.C. Walsh, J. Phys. Chem. B, 109 (2005) 19422

[5] V. Idakiev, Z.Y. Yuan, T. Tabakova, B.L. Su, Appl. Catal. A 281 (2005) 149.

[6] D.V. Bavykin, A.A. Lapkin, P.K. Plucinski, J.M. Friedrich, F.C. Walsh, J. Catal. 235 (2005) 10.

[7] A. Fujishima, T.N. Rao, D.A. Tryk, J. Photochem. Photobiol. C: Photochem. Reviews, 1 (2000) 79.

[8] M.R. Hoffmann, S.T. Martin, W. Choi and D.W. Bahnemann, Chem. Rev. 95 (1995) 69-96.

[9] J.C. Xu, M. Lu, X.Y. Guo, H.L. Lia, J. Mol. Catal. A 226 (2005) 123.

[10] J. Suetake, A.Y. Nosaka, K. Hodouchi, H. Matsubara, Y. Nosaka, J. Phys. Chem. C, 112 (2008) 18474.

[11] K. Nishijima, T. Fukahori, N. Murakami, T. Kamai, T. Tsubota, T. Ohno, Appl. Catal. A: Gen. 337 (2008) 105.

[12] K. Nishijima, Y. Fujisawa, N. Murakami, T. Tsubota, T. Ohno, Appl. Catal. B: Environ. 84 (2008) 584.

[13] N. Murakami, T. Chiyoya, T. Tsubota, T. Ohno, Appl. Catal. A: Gen. 348 (2008) 148.

[14] T. Ohno, N. Murakami, T. Tsubota, H. Nishimura, Appl. Catal. A: Gen. 349 (2008) 70.

[15] N. Murakami, O.O.P. Mahaney, R. Abe, T. Torimoto, B. Ohtani, J. Phys. Chem. C, 111 (2007) 11927-11935.

Figure1

Click here to download high resolution image

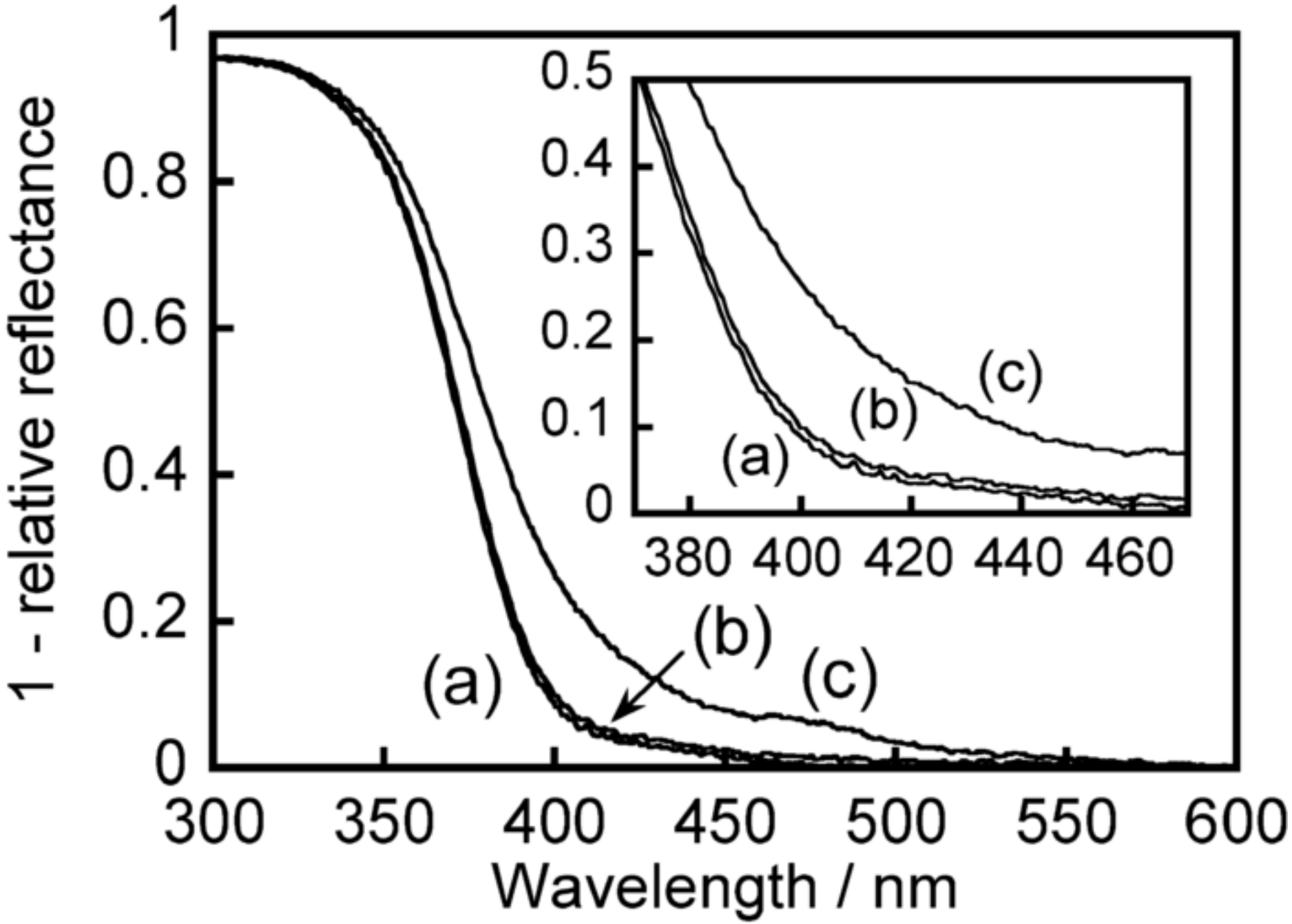

Figure2
Click here to download high resolution image

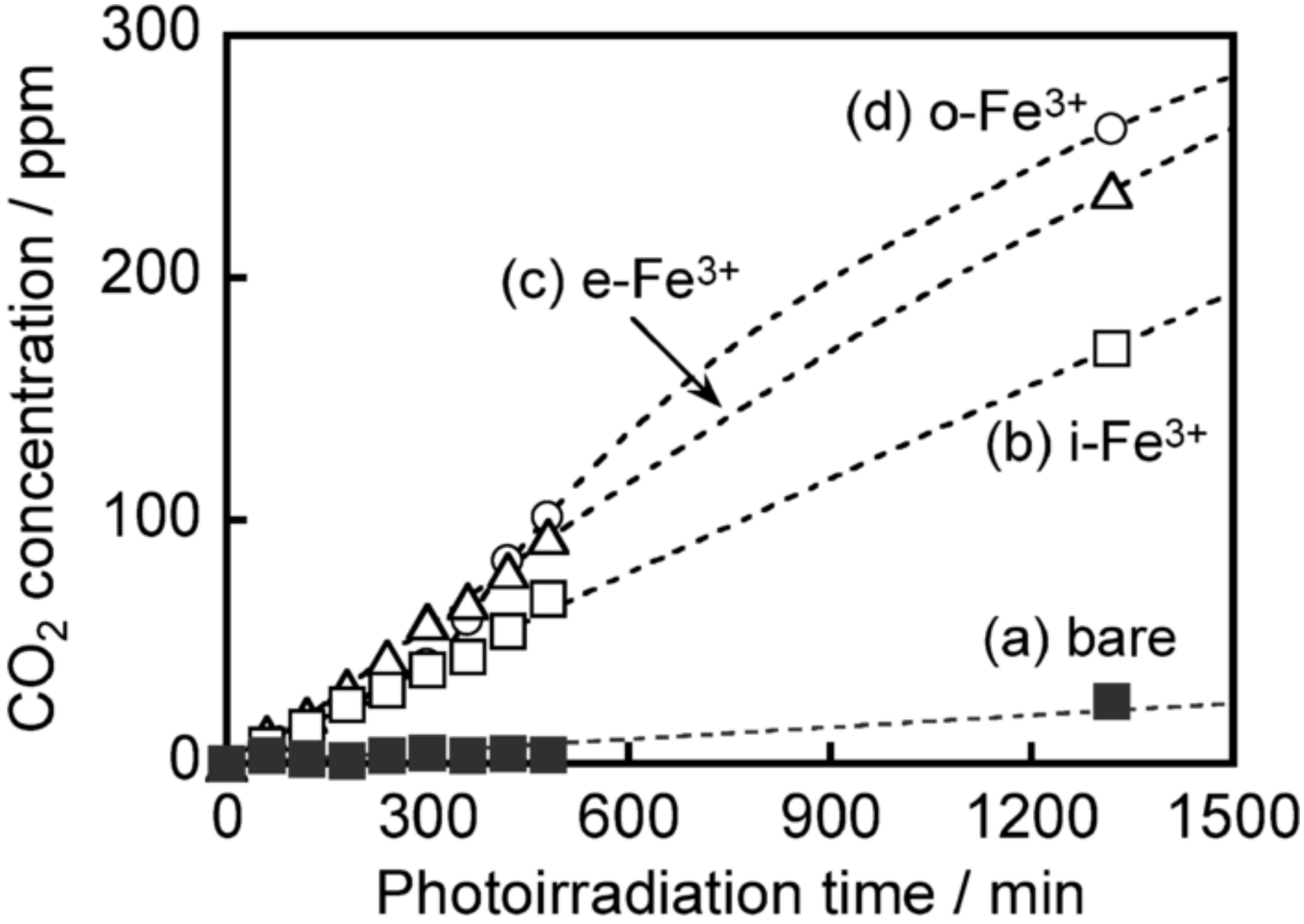

Figure3
Click here to download high resolution image

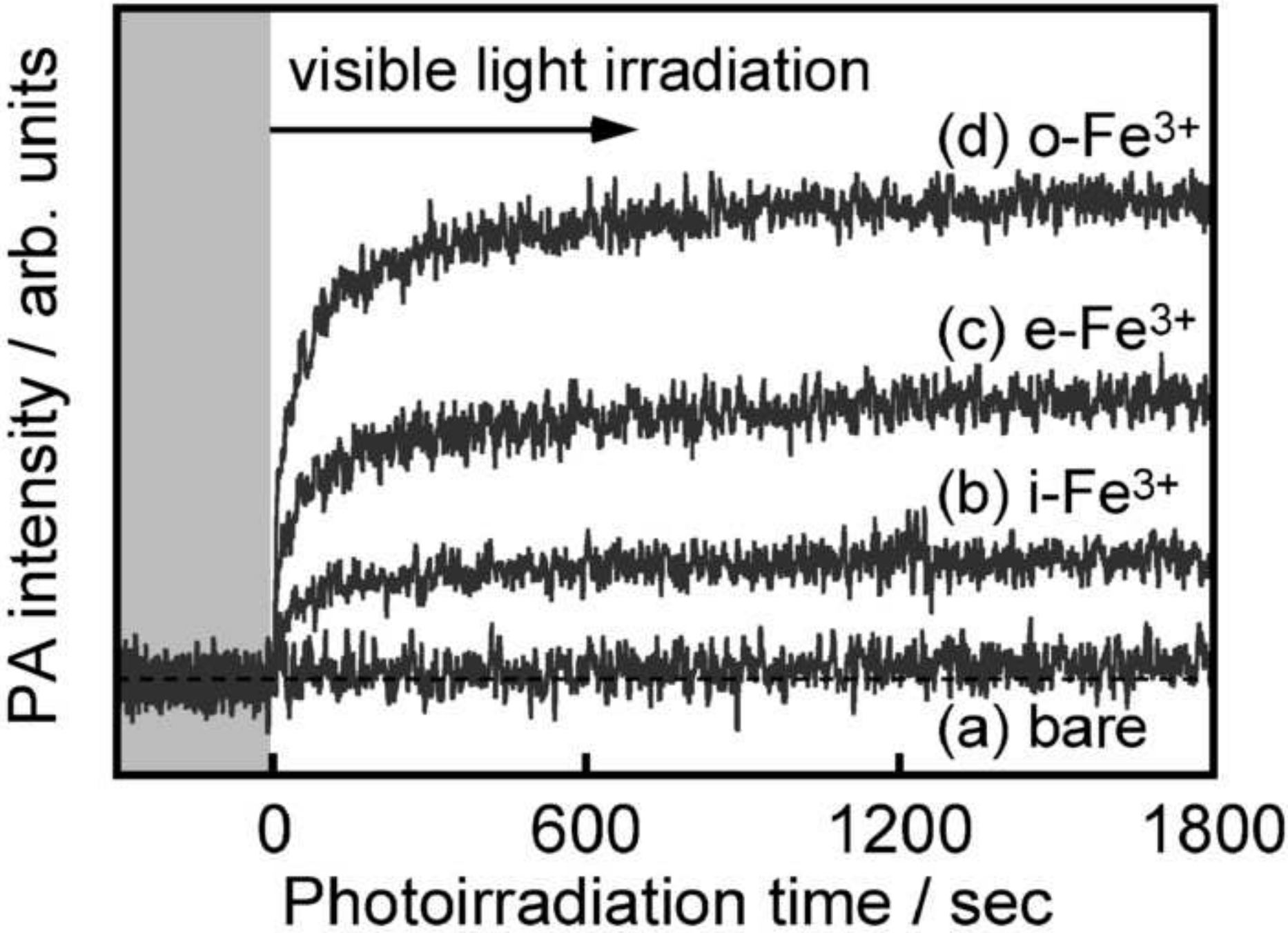

Figure4
Click here to download high resolution image

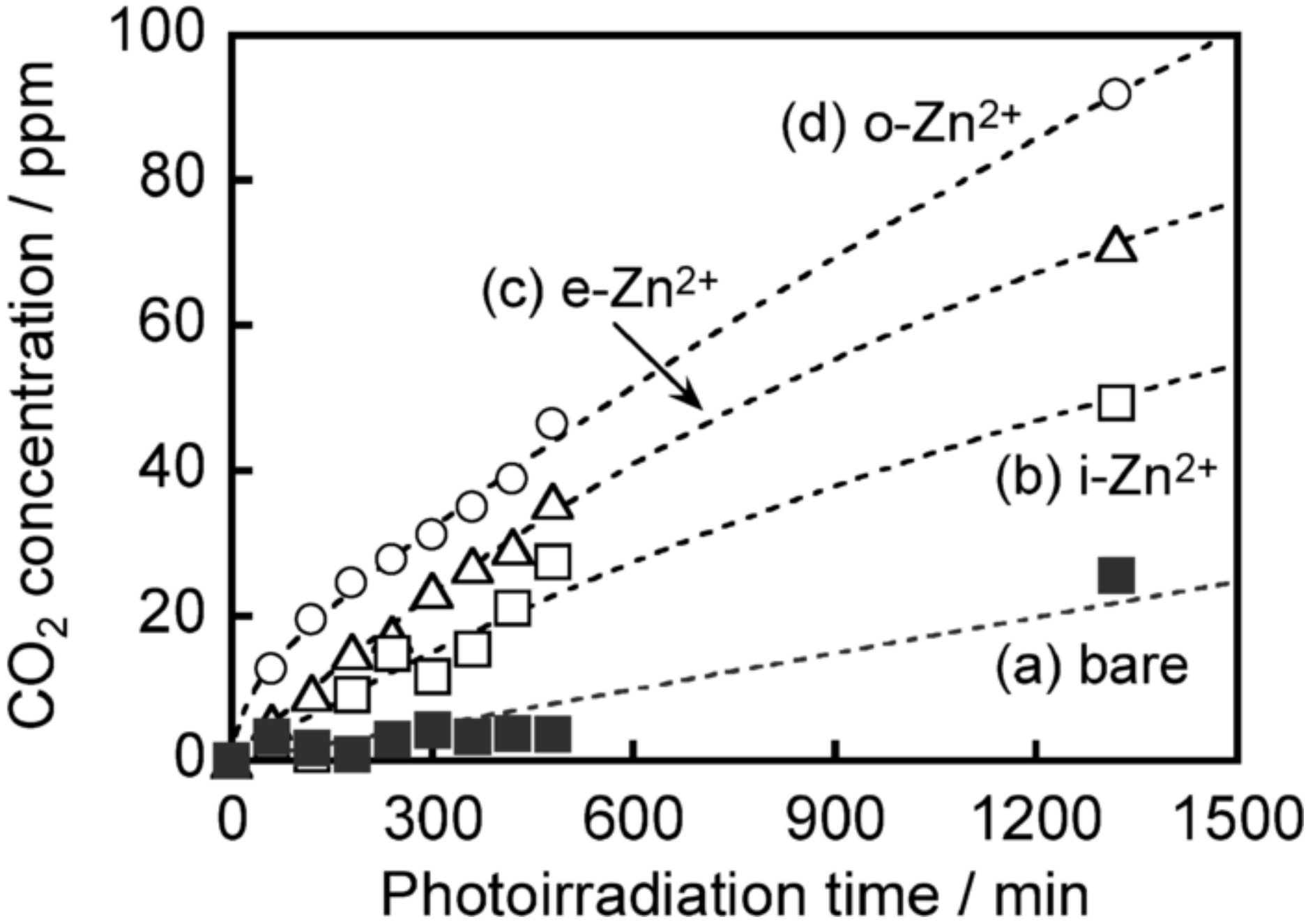

Figure5
Click here to download high resolution image

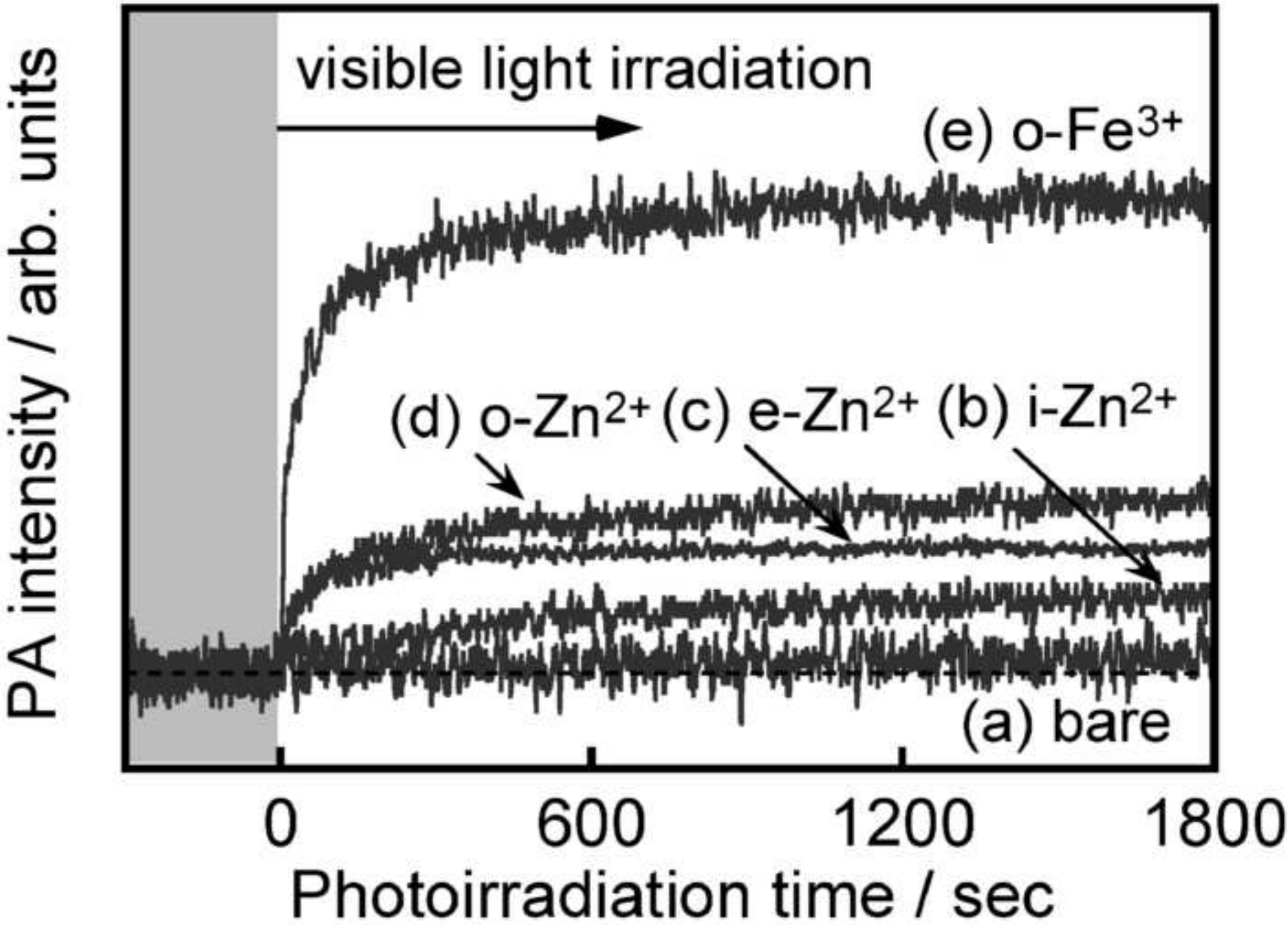

Figure6
Click here to download high resolution image

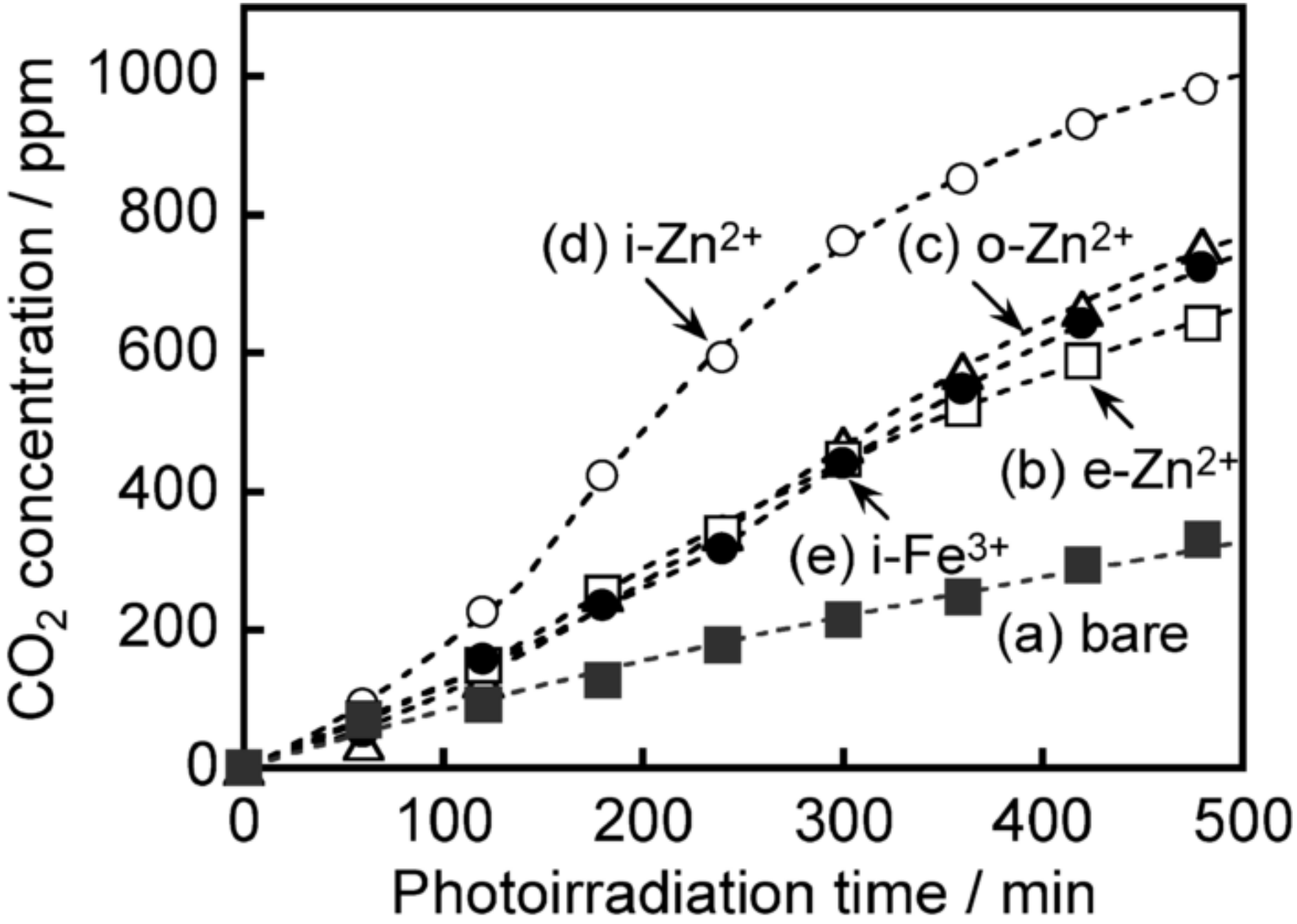

Figure7
Click here to download high resolution image

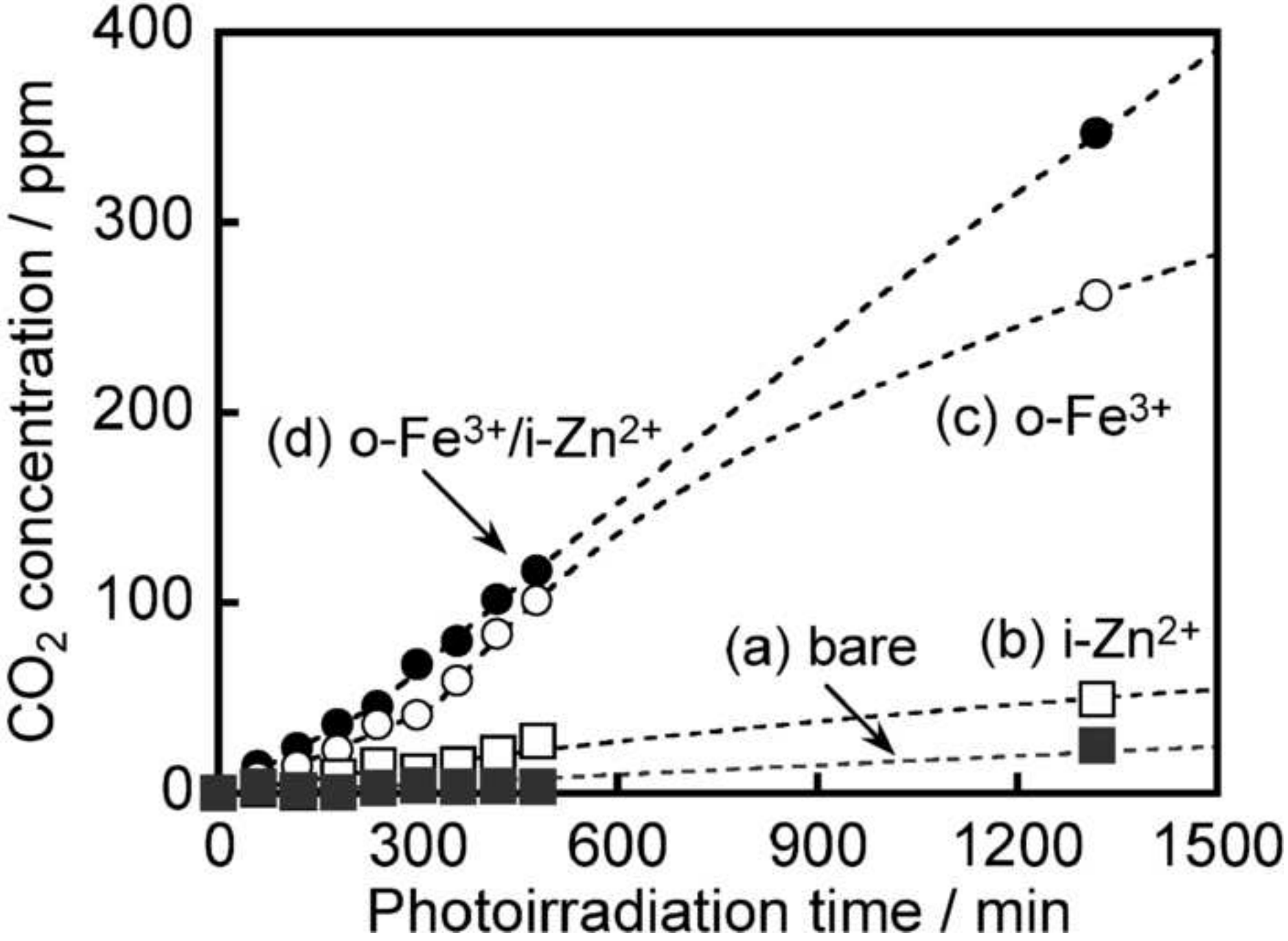

Figure8
Click here to download high resolution image